diversity

MDPI

Article

Widespread Occurrence of Two Planktonic Ciliate Species (*Urotricha*, Prostomatida) Originating from High Mountain Lakes

Bettina Sonntag [1,2,*], Daniela Frantal [1], Barbara Kammerlander [1,2,3], Tatyana Darienko [1,4,5], Sabine Filker [6], Thorsten Stoeck [7], Michael Gruber [8] and Thomas Pröschold [1]

1 Research Department for Limnology, Mondsee, University of Innsbruck, A-5310 Mondsee, Austria; csap5745@gmail.com (D.F.); barbara.kammerlander@baw.at (B.K.); tdarien@gwdg.de (T.D.); thomas.proeschold@uibk.ac.at (T.P.)
2 Ecology Department, University of Innsbruck, A-6020 Innsbruck, Austria
3 Federal Agency for Water Management, Institute for Aquatic Ecology and Fisheries Management, A-5310 Mondsee, Austria
4 Department of Applied Bioinformatics, Institute for Microbiology and Genetics, Georg-August-University Göttingen, D-37077 Göttingen, Germany
5 Experimental Phycology and Culture Collection of Algae, Albrecht-von-Haller-Institute of Plant Sciences, Georg-August-University Göttingen, D-37073 Göttingen, Germany
6 Molecular Ecology Group, Technische Universität Kaiserslautern, D-67663 Kaiserslautern, Germany; filker@rhrk.uni-kl.de
7 Ecology Group, Technische Universität Kaiserslautern, D-67663 Kaiserslautern, Germany; stoeck@rhrk.uni-kl.de
8 Hieronymus-Illustrations, A-5020 Salzburg, Austria; michael_gruber83@hotmail.com
* Correspondence: bettina.sonntag@uibk.ac.at

Abstract: Ciliates of the genus *Urotricha* are widely distributed and occur in almost any freshwater body. Thus far, almost all species have been described from morphology only. Here, we applied an integrative approach on the morphology, molecular phylogeny and biogeography of two species isolated from high mountain lakes in the Central Alps, Austria. As these remote lakes are known to have water temperatures <15 °C, our hypothesis was that these urotrichs might prefer 'cold' environments. We studied the morphological details from living and silver-stained individuals, and their molecular sequences (ribosomal operon, ITS), and screened available datasets for their biogeography. The two *Urotricha* species resembled morphological features of several congeners. An accurate species assignment was difficult due to several overlapping characteristics. However, we tentatively attributed the investigated species to *Urotricha nais* and *Urotricha globosa*. The biogeographic analyses revealed their occurrence in Europe, Africa and Asia, and no correlations to (cold) temperatures were found. Our findings suggest that these two urotrichs, originating from two cold and remote habitats, are probably cryptic species well adapted to their harsh environment.

Keywords: protists; microbial food web; alpine lakes; biogeography; taxonomic marker genes; cryptic species

Citation: Sonntag, B.; Frantal, D.; Kammerlander, B.; Darienko, T.; Filker, S.; Stoeck, T.; Gruber, M.; Pröschold, T. Widespread Occurrence of Two Planktonic Ciliate Species (*Urotricha*, Prostomatida) Originating from High Mountain Lakes. *Diversity* **2022**, *14*, 362. https://doi.org/10.3390/d14050362

Academic Editor: Hongbin Liu

Received: 8 April 2022
Accepted: 1 May 2022
Published: 4 May 2022

1. Introduction

Urotricha species belong to the most important ciliates in freshwater lake ecosystems [1]. They consume a considerable amount of the phytoplankton biomass during the spring bloom in temperate lakes together with other prostomatid and oligotrich ciliate species [2]. In planktonic microbial food webs, some species were recently identified as key players pointing to their omnivorous feeding mode that underlines their flexibility in exploiting various food resources [3]. Especially small *Urotricha* species <40 µm are predominantly found in diverse water bodies in high numbers; however, their morphological identification is rather difficult [1]. In alpine lakes, i.e., above the tree-line and also in man-made mountain reservoirs located at high altitudes, urotrichs are regularly detected in the plankton [4–8].

Moreover, their occurrence in relatively young water bodies such as man-made mountain reservoirs suggests that they might be primary settlers in high-altitude lakes [8].

Here, we isolated two *Urotricha* species from two high mountain lakes in the Austrian Central Alps and our hypothesis was that these *Urotricha* species do not tolerate water temperatures exceeding 15 °C, which is the maximum temperature known for alpine lakes [9]. We screened 'environmental sequences' deposited in public databases (e.g., NCBI) and worldwide high throughput sequencing (HTS) datasets for the occurrence of the two species. Moreover, we correlated available abiotic parameters along with the HTS datasets to verify our hypothesis. Additionally, as taxonomic datasets on urotrichs in general and on small species <40 µm in particular are scarce, we present detailed morphological analyses and their species-specific molecular sequences including the usage of the conserved region of the ITS-2 as a barcode marker for *Urotricha*.

2. Materials and Methods

2.1. Sampling Sites, Sampling, Cultivation and Identification of the Ciliates

Plankton samples containing the desired *Urotricha* species were collected in two alpine lakes located above the tree-line in the Austrian Central Alps. Details on Lake Hairlach and Lake Faselfad (i.e., FAS 5) can be found elsewhere [6,7,10]. Briefly, water samples were taken with a 5-L Schindler-Patalas sampler (Uwitec) both as depth-specific and 10-µm net-samples over the respective deepest point of a lake. Samples containing living ciliates were transported in 1-L plastic bottles at ambient lake water temperatures to the laboratory and investigated within 24 h. For subsequent ciliate staining by diverse quantitative and qualitative protargol methods [11,12], raw water from the sampler and clone cultures (see details below) were preserved with freshly prepared Bouin's solution (5% final conc.). Morphological details of the urotrichs were studied from living and protargol-stained individuals, and some of the latter were also drawn with a camera lucida from permanent slides [11]. Living cells were studied under differential interference contrast at magnifications of up to 1000× with an Olympus BX51 microscope (Olympus, Vienna, Austria). Stained specimens were investigated with brightfield contrast. The urotrichs were identified following the keys of Foissner et al. [13,14] and after Frantal et al. [1]. Images were taken with two digital cameras connected to the microscope (Jenoptik ProgRes Speed XT core 5 2.9.0.1., Jenoptik PROGRES Gryphax (R) Arktur). Measurements were performed with the same image analysis systems or with a calibrated eyepiece micrometer. Measurements and counts of morphometric features were performed on 21 cells maximum as is standard in ciliate taxonomy.

Ciliate cultivation and sequencing followed the methods described in Frantal et al. [1]. Briefly, ciliates were individually picked from a sample, cleaned over several drops of sterile medium and starved to get rid of ingested (other protist) food that may have contaminated the sequencing products. Then, individual cells were subjected to clone cultures and single-cell sequencing.

2.2. Molecular Methods and Phylogenetic Analyzes

The starved cells as described above were used for genome replication with the REPLI-g kit (Qiagen, Hilden, Germany; for detailed description, see [1]). The PCR was conducted with two primer combinations (EAF3/CilR and CilF/ITS055R; [1]) followed by PCR purification using the QIAquick PCR purification kit (Qiagen, Hilden, Germany). The sequencing results showed multiple bands in the ITS region of both *Urotricha* strains. Therefore, the PCR of the CilF/ITS055R combination was repeated and the products were purified using the QIAquick Gel Extraction Kit (Qiagen, Hilden, Germany). The purified PCR products were cloned into competent *E. coli* cells using the TOPO TA cloning Kit (Invitrogen, Carlsbad, CA, USA). The cloning procedure was conducted using the following protocol: (i) 2 µL of purified PCR product was gently mixed with the ligation mixture of 1 µL TOPO vector 4, 1 µL salt solution and 2 µL of sterile H_2O (all provided in the kit). This mixture was incubated for 5 min at room temperature. (ii) Two µL of the

ligation mixture was added to 50 µL of OneShot-Top10 competent *E. coli* cells, gently mixed, and then incubated for 5 min on ice. The cells were then incubated for 35 sec at 42 °C without shaking, transferred on ice and immediately, 250 µL SOC medium was added. The cells were then shaken at 150 rpm for 1 h at 37 °C. (iii) Next, 20, 40 and 60 µL of the transformed cells were placed onto separate LAX plates and gently spread. The plates were incubated for 16–18 h at 37 °C. The LAX medium was prepared as follows: to 1 L water, 10 g Bacto-tryptone (Difco), 5 g Yeast extract (Difco), 5 g NaCl and 13 g agar were added, mixed and autoclaved. After cooling down, 2 mL X-Gal (Sigma-Aldrich; 40 mg/mL) and 1 mL ampicillin (Sigma-Aldrich; 100 mg/mL) were added. (iv) White colonies grown on the plates were collected with sterile toothpicks and transferred to new LAX plates and incubated for further 16 h at 37 °C. In addition, the rest of the colonies was picked with toothpicks and added to 50 µL of the prepared PCR mix using the CilF/ITS055R combination. The PCR was conducted under the same conditions and the PCR products were purified as described above. After sequencing, the SSU and ITS sequences were included into the datasets of the urotrichs analyzed in [1].

To prove that both isolates belonged to the genus *Urotricha*, we analyzed the SSU dataset of 23 taxa (1755 bp) using the same methods described in detail in Frantal et al. [1]. As demonstrated in Figure S1 (Supplementary Materials), both strains belonged to the genus *Urotricha*. Consequently, the SSU and ITS sequences were included into the SSU/ITS dataset (20 taxa, 2375 bp) and analyzed using the same programs as described in Frantal et al. [1]. The analyses were conducted using PAUP version 4.0a169 [15], RAxML [16] and PHASE [17–21]. The settings of the best models according to the Akaike Information Criterion are provided in the figure legends.

The secondary structures of the hypervariable V4 and V9 regions (SSU), commonly used for DNA metabarcoding, were folded using the program *mfold* [22] and visualized with PseudoViewer3 [23].

2.3. ITS-2 Secondary Structures and ITS-2/CBC Approach

For folding of the ITS-2 sequences, two computer programs were used: *mfold* [22], which used the thermodynamical model (minimal energy), and *CONTRAfold* [24], another program that applied a stochastic approach for RNA folding. Three constraints were set for the folding: (i) the last 20 bases of the 5.8S rRNA and the first 20 of the LSU rRNA must have bound and formed the 5.8S/LSU stem (to avoid analyzing pseudogenes), (ii) the pyrimidine/ pyrimidine mismatch (the first RNA processing site) in Helix II after the 4th–6th base pair had to be present in the structure and, (iii) the second RNA processing site, the GGUCACU motif as it is characteristic for the Prostomatea, had to be located at the 5′ site in Helix III (for details about the processing sites and constraints, see [25–27].

The ITS-2 secondary structure models derived from these foldings were used for species delimitation among all investigated *Urotricha* strains. For the Prostomatea, only three helices could be discovered, which corresponded to helices II-IV of the model provided by Coleman [28]. Helix I is missing in ciliates. The ITS-2/CBC approach introduced for the green algal genus *Coccomyxa* by Darienko et al. [29] was applied here for the ciliates. This approach used the conserved region of the ITS-2, which includes 16 base pairs of the 5.8S/LSU stem, seven base pairs of Helix II including the pyrimidine–pyrimidine mismatch, and all base pairs of Helix III. The resulting dataset was manually aligned according to the secondary structures. These alignments were translated into base pair alignment by usage of a number code for each base pair (1 = A-U; 2 = U-A; 3 = G-C; 4 = C-G; 5 = G•U; 6 = U•G; 7 = mismatch; 8 = deletion/insertion or single bases). These barcodes of each species were compared to detect compensatory base changes (CBCs), hemi-CBCs (HCBCs) and/or insertion/deletion, single or unpaired bases.

2.4. Screening for Ciliate Biogeography and Correlation to Abiotic Lake Water Parameters

For the occurrence of the two urotrichs in HTS datasets, we screened a European lake dataset (V9; [3,30,31]), a high mountain lake dataset, including lakes from Austria, Ethiopia

and Chile (V4; [32]), as well as two high mountain lakes located in the Himalaya (V4; [10]; Table S1).

3. Results

3.1. Identification of the Urotrichs

From their sequences, both urotrichs can be clearly distinguished from other small species presented in Frantal et al. [1] and they cluster with the *Urotricha agilis* complex (Figures 1–3). Because the two species resembled morphological features of several other small *Urotricha* congeners having only one caudal cilium (see summary table in the discussion), we primarily relied on relatively stable characteristics, i.e., the number of somatic kineties, to tentatively assign our species to *Urotricha nais* and *Urotricha globosa*, respectively, rather than incorporating them into the *U. agilis* complex. The two species can morphologically be distinguished from other congeners (see below), but the original descriptions are often insufficient to find a matching morphotype (see summary table in the discussion). However, in the following, we give detailed descriptions of the morphotypes of the two urotrichs analyzed in this study.

Urotricha nais Muñoz, Téllez and Fernández-Galiano, 1987 from Lake Faselfad (Figures 1 and 2; Table S2).

The cell is ellipsoidal to broadly ellipsoidal in the frontal half in vivo and in protargol stained cells. It measures 17–35 × 15–29 µm in vivo and 10–18 × 8–15 µm in protargol preparations. The cell length:width ratio is 1.1–1.5:1 in vivo and in protargol preparations. The unciliated posterior cell portion is not set off plug-like and occupies 24–34%, on average 29% of cell length, being 3–5 µm long in protargol preparations. The globular to broadly ellipsoidal macronucleus measures 4–11 × 4–11 µm in vivo and 4–7 × 3–5 µm in protargol preparations; the almost globular micronucleus measures 1–3 × 1–5 µm in vivo and 1–2 × 1–2 µm in protargol preparations. The rod-shaped somatic extrusomes are about 1–3 µm long and hardly visible in vivo and about 1 µm long in protargol preparations where they are conspicuously stained. The cytoplasm is colorless and includes refractive lipid droplets 1–2 µm across and often many (colorful) food vacuoles of 2–8 µm, on average 5 µm across. The contractile vacuole is up to 6 µm across. The somatic cilia are relatively long with 4–7 µm in vivo and 4–6 µm in protargol preparations. The somatic ciliature comprises 15–19 kineties consisting of 8–11 cilia in anteriorly unshortened rows. The length of the single caudal cilium is about half the cell length, namely 7–17 µm long in vivo and 5–11 µm long in protargol preparations. The oral basket is 3–5 µm across distally and occupies 28–54% and 39% on average in protargol preparations. The most probably two adoral organelles ('brosse') are inconspicuous: adoral organelle one consists of four dikinetids and adoral organelle two consists of two dikinetids.

Urotricha globosa (Schewiakoff, 1892) Song and Wilbert, 1989 from Lake Hairlach (Figures 1 and 2, Table S2).

The cell is ellipsoidal to broadly ellipsoidal in vivo and in protargol stained cells. It measures 11–17 × 9–15 µm in protargol preparations. The cell length:width ratio is 1.1–1.4:1 in protargol preparations. The unciliated posterior cell portion is not set off plug-like and occupies 19–45%, on average 33% of cell length, being 3–7 µm long in protargol preparations. The globular to broadly ellipsoidal macronucleus measures 3–6 × 2–5 µm in protargol preparations; the almost globular micronucleus measures 1–2 × 1–2 µm in protargol preparations. The rod-shaped somatic extrusomes are about 1–1.5 µm long in protargol preparations where they are conspicuously stained; they are arranged between the ciliary rows mainly in the ciliated cell portion, sometimes with one conspicuous dense horizontal row at the posterior end of the somatic cilia; moreover, they are additionally found in a loose vertical pattern in the unciliated posterior end of the cell; other shorter extrusomes of about 1 µm in length are densely arranged around the oral region. The cytoplasm is colorless and includes refractive lipid droplets and often many (colorful) food vacuoles. The somatic cilia are relatively long with 4–6 µm in protargol preparations. The somatic ciliature comprises 16–24 kineties consisting of 5–8 cilia in anteriorly unshortened

rows. The length of the single caudal cilium is about one third to half the cell length, namely 3–7 µm long in protargol preparations. The 8–13 oral flaps are 1.5–2.0 µm long in protargol preparations. The oral basket is 3–5 µm across distally and occupies 25–44% and 33% on average in protargol preparations; the oral basket is 5–10 µm long in protargol preparations. The most probably two adoral organelles ('brosse') are inconspicuous: adoral organelle one consists of four dikinetids and is 2 µm in length, adoral organelle two consists of two dikinetids and is 1 µm in length. They are placed in a comparatively broad (about 1.4 µm on average) blank stripe, which separates the circumoral kinety and the somatic kineties.

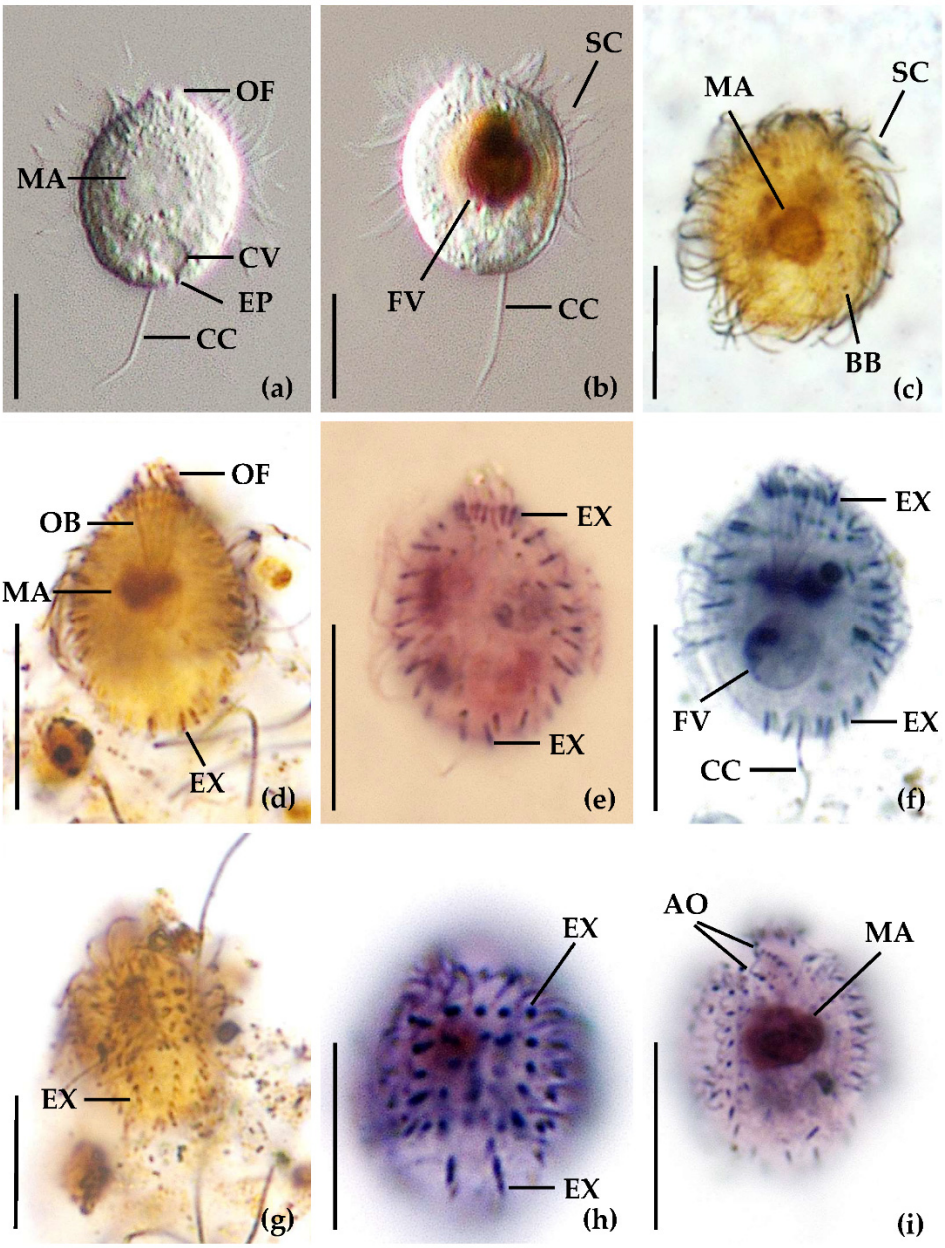

Figure 1. Species tentatively assigned to *Urotricha nais* from Lake Faselfad (**a**–**c**) and *Urotricha globosa* from Lake Hairlach (**d**–**i**) in vivo from the non-clonal original culture (**a**,**b**) and after protargol staining (**c**–**i**). (**a**–**i**) Longitudinal optical sections. (**e**–**h**) Extrusomes are aligned along the ciliary rows around mid-cell and in the unciliated posterior portion in characteristic vertical rows. (**g**,**h**) Specific extrusomes are arranged around the anterior part of the oral basket (**e**,**f**). (**i**) Details of the adoral organelles. AO—adoral organelles, BB—basal bodies of a somatic kinety, CC—caudal cilium, CV—contractile vacuole, EP—excretory pore of the contractile vacuole, EX—extrusomes, FV—food vacuole, MA—macronucleus, OB—oral basket, OF—oral flaps, SC—somatic cilia. Scale bars 10 µm.

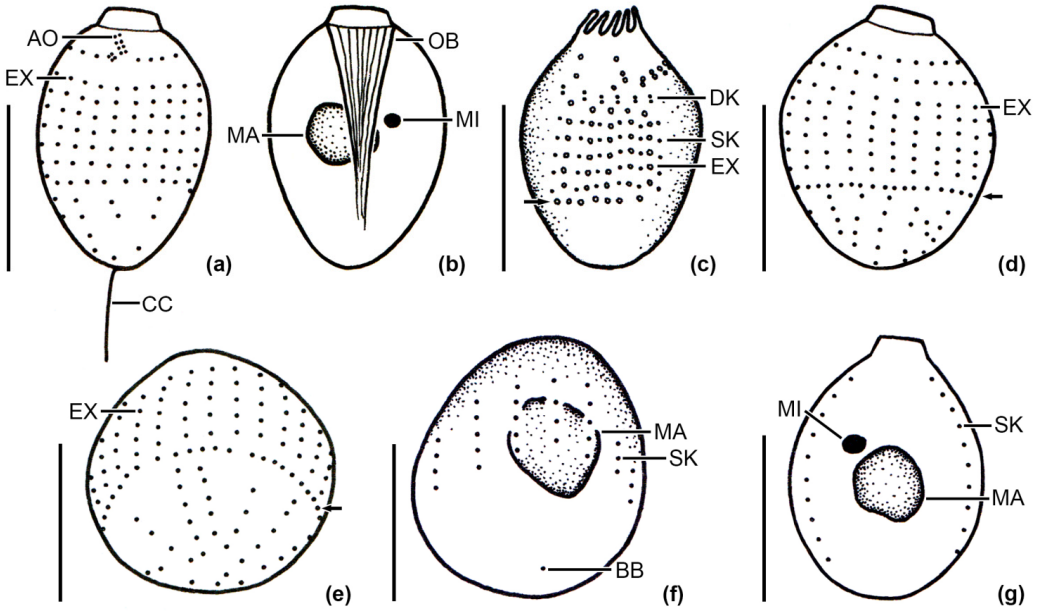

Figure 2. Species tentatively assigned to *Urotricha globosa* from Lake Hairlach (**a**–**e**) and *Urotricha nais* from Lake Faselfad (**f**,**g**) after protargol staining. (**a**,**d**,**e**). Ventral, dorsal and oblique posterior polar views. Note that the extrusomes and not the basal bodies of the ciliary rows are shown except for the adoral organelles and the caudal cilium in (**a**). Extrusomes are arranged longitudinally between the ciliary rows and in vertical rows in the unciliated posterior portion (**e**); note the horizontally more densely arranged extrusomes at the end of the ciliated area (arrows) in (**c**–**e**). (**b**) Optical section showing the anterior protruding oral region and the nuclei. (**c**). Details of the cell cortex showing the extrusomes (illustrated by circles) located between the somatic kineties (exemplarily, only a section of the total ciliature is shown). (**f**,**g**) Details of the infraciliature and nuclei; note that in (**f**) not the total length and the correct number of basal bodies of the somatic kineties is shown and in the schematic overview in (**g**), only two somatic kineties are exemplarily shown. AO—adoral organelles, BB—basal body of the single caudal cilium, CC—caudal cilium, DK—dikinetids at anterior end of somatic kineties, EX—extrusomes, MA—macronucleus, MI—micronucleus, OB—oral basket, SK—somatic kineties. Arrows denote singular dense extrusome row at the posterior end of the somatic ciliary rows in *Urotricha globosa*. Scale bars 10 μm.

3.2. Molecular Phylogeny

Phylogenetic analyses assigned both strains unambiguously to the genus *Urotricha* (Figures 3 and S1). Both species identified as *U. nais* and *U. globosa* are closely related to the *U. agilis* complex in the phylogeny using the concatenated dataset of SSU and ITS rDNA sequences. The tree topology was highly supported in all bootstrap analyses (Figure 3). As already demonstrated in [1], the species of *Urotricha* could be clearly distinguished by the V4 region of the SSU, but not by the V9. Therefore, we compared the secondary structures of both regions to confirm that both investigated strains could also be identified by those regions. Both species showed clear synapomorphies in the V4, which are highlighted in white boxes in Figure 4. In contrast, the V9 of *U. globosa* and *U. agilis* were identical, confirming the close relationship between both species (Figure S2). Both regions, V4 and V9, commonly used in environmental DNA metabarcoding studies, showed different diagnostic power for species discrimination. To elucidate the species discriminatory thresholds of both taxonomic DNA marker regions, we compared them pairwise. Despite similar variability in both regions (V4: 40 of 218 bp—18.3%; V9: 18 of 98 bp—18.4%), the uncorrected p-distance matrix of the V4 revealed a threshold of 2% for distinguishing species within the genus *Urotricha* (Table 1). In contrast, the V9 of *U. agilis*/*U. globosa* and *U. furcata*/*U. pseudofurcata* were identical. Therefore, this region is only group- and not species-specific.

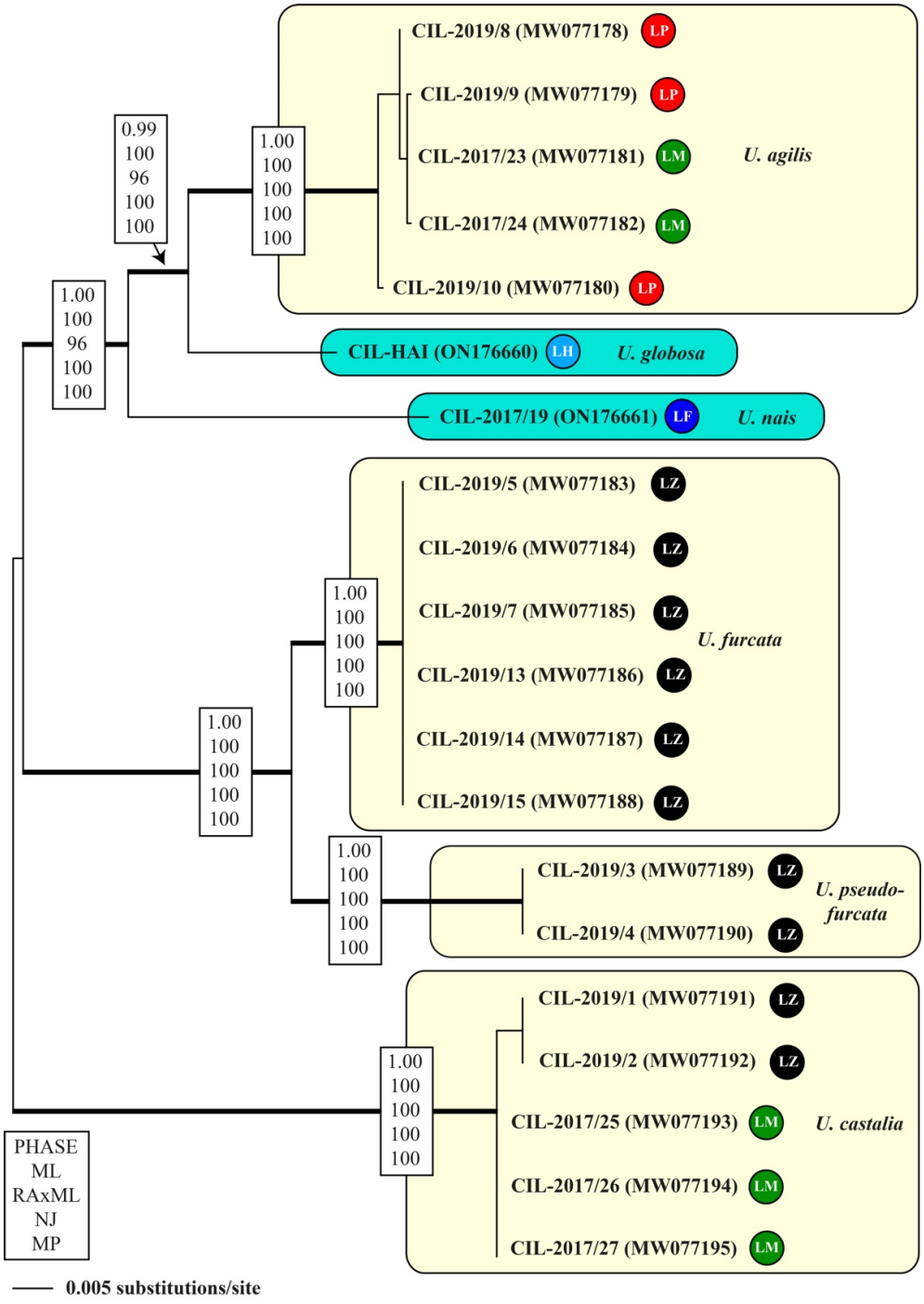

Figure 3. Molecular phylogeny of the genus *Urotricha* inferred from SSU and ITS rDNA sequences, using the maximum likelihood method of PAUP 4.0a169 on a dataset with 2375 aligned positions of 20 taxa. For the analyzes, the best model was calculated with automated model selection tool implemented in PAUP. The setting of the best model was given as follows: GTR + I + G (base frequencies: A 0.3053, C 0.1670, G 0.2126, U 0.3151; rate matrix A-C 1.5642, A-G 2.1281, A-U 3.3467, C-G 0.5508, C-U 4.1562, G-U 1.0000) with the proportion of invariable sites (I = 0.6293) and gamma shape parameter (G = 0.6791). The branches in bold are highly supported in all bootstrap analyses (Bayesian values >0.95 and bootstrap values >50% calculated with PHASE, PAUP and RAxML, using the maximum likelihood, neighbor joining and maximum parsimony, respectively). The colored circles following the strain designation indicate the strain origins (LP = Lake Piburg; LM = Lake Mondsee; LH = Lake Hairlach; LF = Lake Faselfad, all Austria; LZ = Lake Zurich, Switzerland).

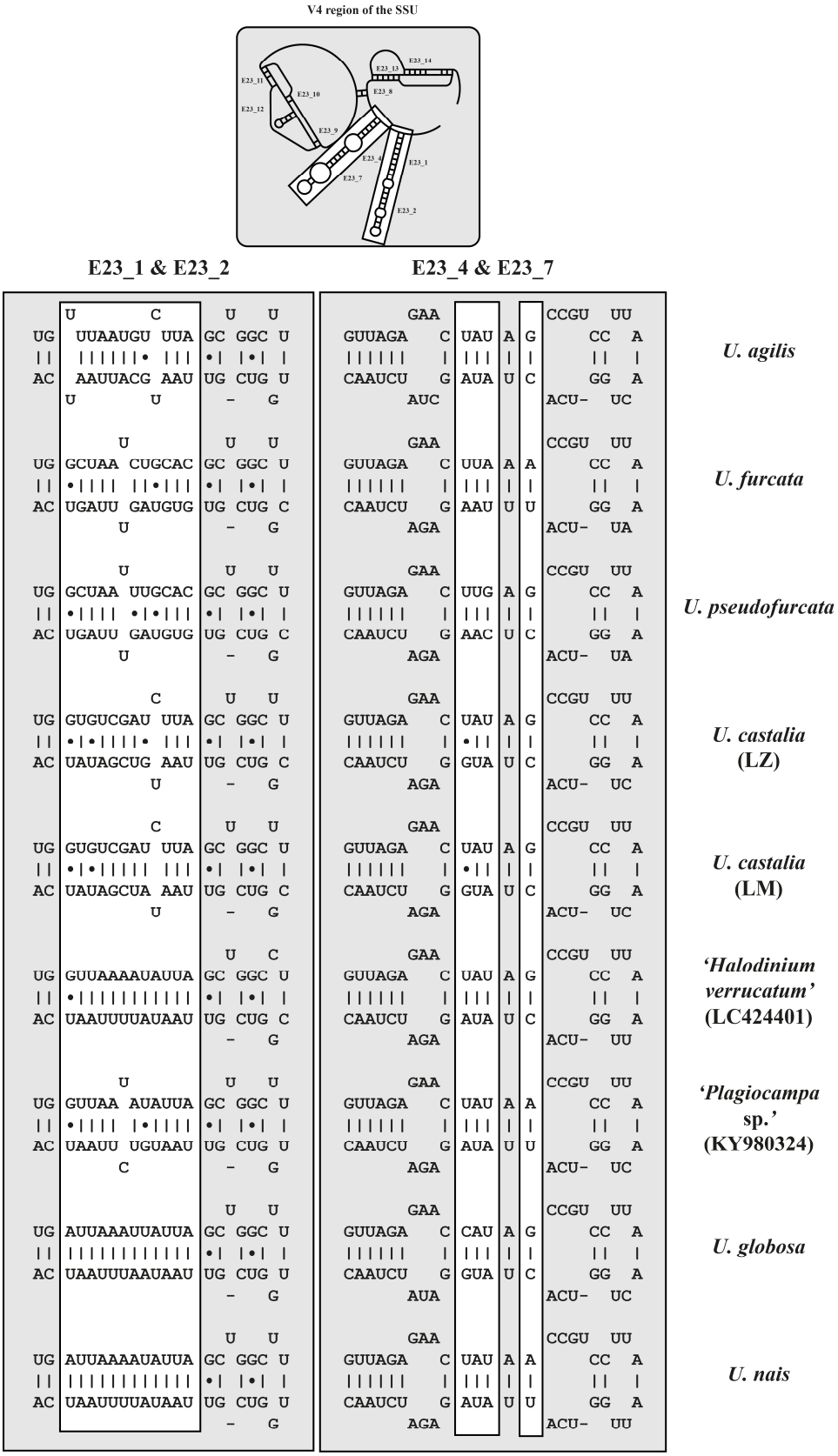

Figure 4. V4 secondary structures of the investigated *Urotricha* strains. The variable regions are marked by white boxes. The structures of E23_1/E23_2 and E23_4/E23_7 were calculated with *mfold*. The line graphic was drawn with PseudoViewer. LM, Lake Mondsee population; LZ, Lake Zurich population.

Table 1. Pairwise comparison of V4 and V9 region among the *Urotricha* species. Bottom left: uncorrected p-distance matrix calculated with PAUP version 4.0a169, upper left: number of base differences in pairwise comparison.

	V4 (218 bp)	1	2	3	4	5	6	7	8	9
1	*U. agilis*	-	10	12	26	24	18	19	12	10
2	*U. globosa*	0.04587	-	8	26	23	19	18	9	12
3	*U. nais*	0.05505	0.03670	-	21	23	19	18	5	6
4	*U. furcata*	0.11927	0.11927	0.09633	-	5	33	32	22	22
5	*U. pseudofurcata*	0.11009	0.10550	0.10550	0.02294	-	31	30	20	24
6	*U. castalia* (LZ)	0.08257	0.08716	0.08716	0.15138	0.14220	-	1	16	16
7	*U. castalia* (LM)	0.08716	0.08257	0.08257	0.14679	0.13761	0.00459	-	15	17
8	*Halodinium*	0.05505	0.04128	0.02294	0.10092	0.09174	0.07339	0.06881	-	9
9	*Plagiocampa*	0.04587	0.05505	0.02752	0.10092	0.11009	0.07339	0.07798	0.04128	-
	V9 (98 bp)	1	2	3	4	5	6	7	8	9
1	*U. agilis*	-	0	5	10	10	11	12	6	7
2	*U. globosa*	0.00000	-	5	10	10	11	12	6	7
3	*U. nais*	0.05102	0.05102	-	11	11	14	13	4	5
4	*U. furcata*	0.10204	0.10204	0.11224	-	0	11	10	12	11
5	*U. pseudofurcata*	0.10204	0.10204	0.11224	0.00000	-	11	10	12	11
6	*U. castalia* (LZ)	0.11224	0.11224	0.14286	0.11224	0.11224	-	1	13	12
7	*U. castalia* (LM)	0.12245	0.12245	0.13265	0.10204	0.10204	0.01020	-	12	11
8	*Halodinium*	0.06122	0.06122	0.04082	0.12245	0.12245	0.13265	0.12245	-	3
9	*Plagiocampa*	0.07143	0.07143	0.05102	0.11224	0.11224	0.12245	0.11224	0.03061	-

To confirm the species conception within the genus *Urotricha*, we compared the ITS-2 secondary structures. The ITS-2 secondary structures of *U. globosa* (Figure 5) and *U. nais* (Figure 6) showed the ciliate typical helices II–IV containing both RNA processing sites highlighted in boxes. In addition, we applied the ITS-2/CBC approach for all species of the genus *Urotricha* (Figure 7). All species could be differentiated by a unique ITS-2 barcode (provided as number code in Figure 7) and the pairwise comparison revealed compensatory base changes for each species.

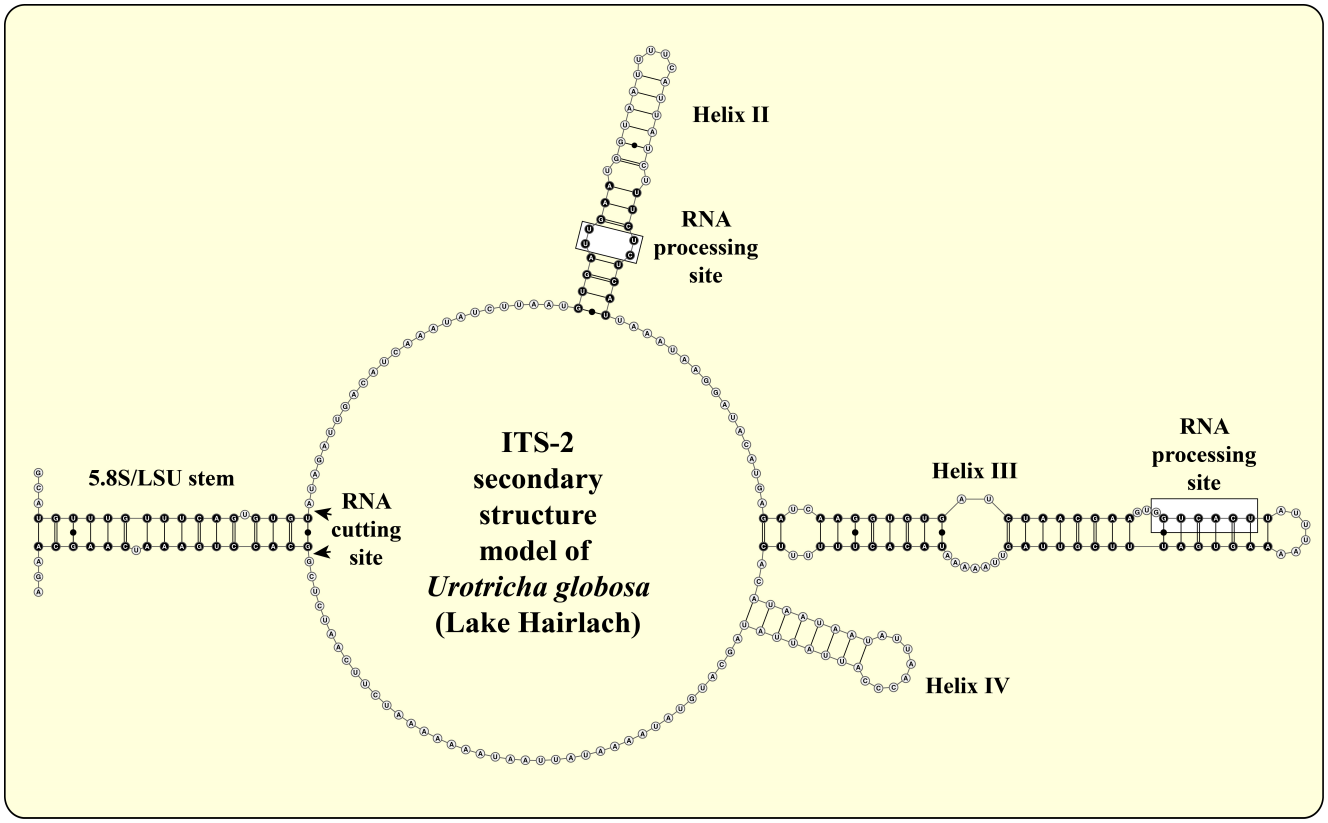

Figure 5. ITS-2 secondary structure of *Urotricha globosa.* Bases marked in black circles were used for the ITS-2/CBC approach. The RNA processing sites are highlighted in white boxes.

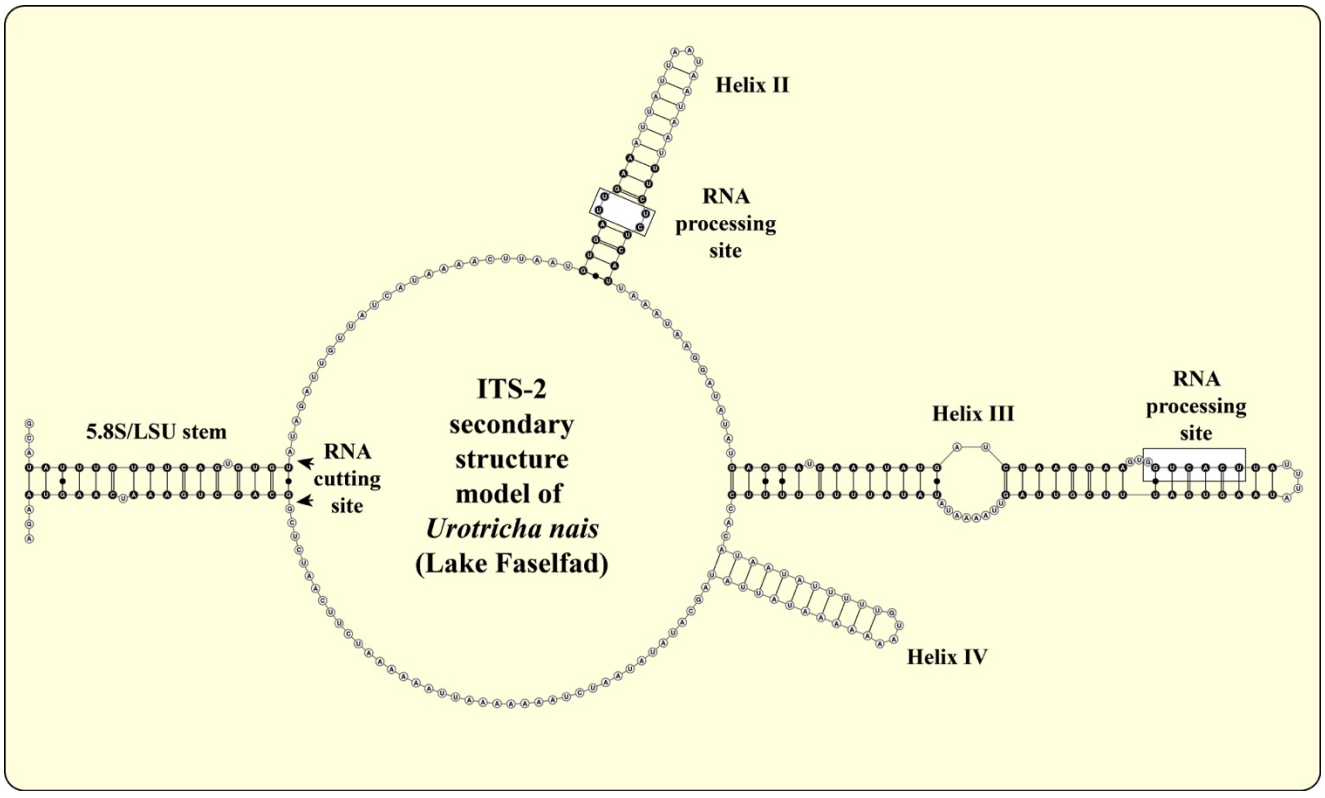

Figure 6. ITS-2 secondary structure of *Urotricha nais*. Bases marked in black circles were used for the ITS-2/CBC approach. The RNA processing sites are highlighted in white boxes.

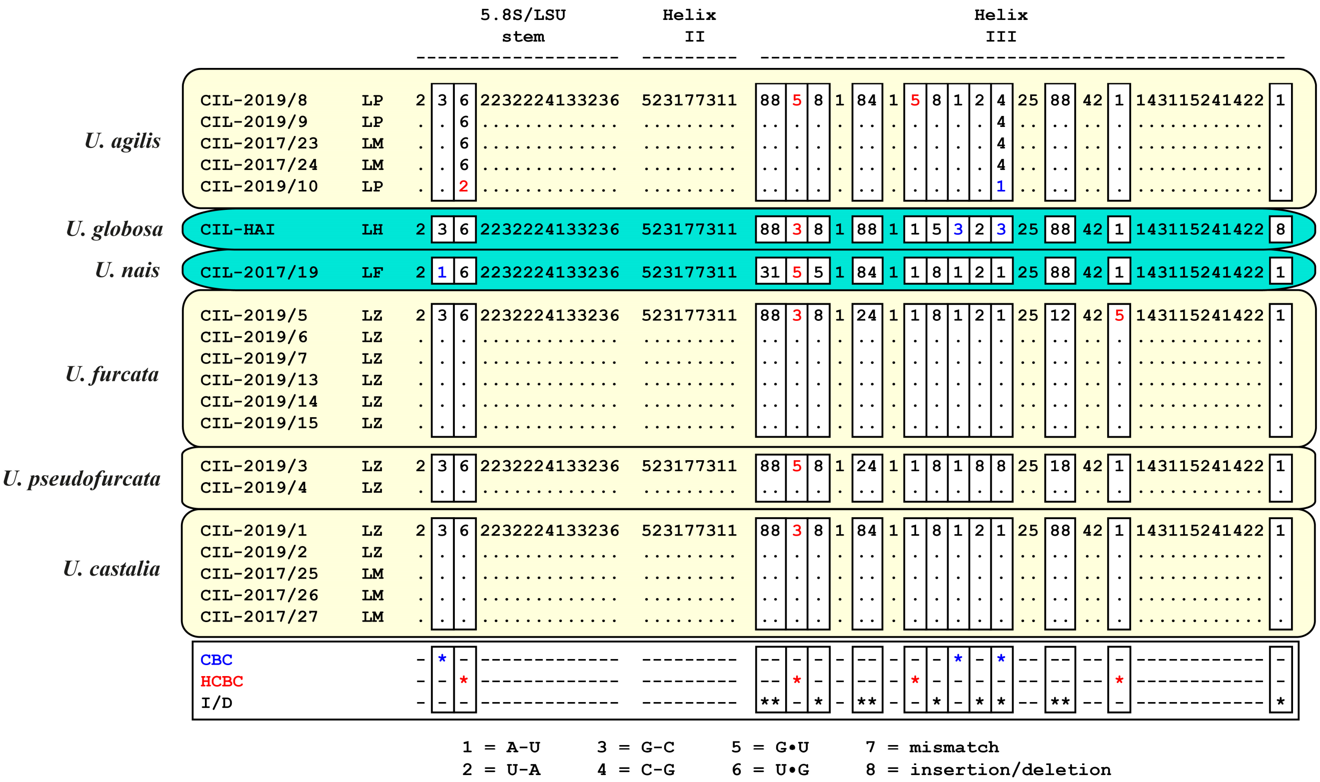

Figure 7. Comparison of the conserved region of ITS-2 among the species of *Urotricha* translated into number codes used as barcodes. Differences among the species are highlighted in white boxes.

3.3. Biogeography and Correlations to Abiotic Environmental Datasets

In the freshwater lakes screened for the presence of the two urotrichs' V4 and V9 barcode markers, we found them occurring in almost all investigated countries except for Chile, the Czech Republic, Iceland and Slovakia (Figure 8, Table S3). Significant correlations ($p < 0.05$) of the two urotrichs with individual ions, conductivity, SO_4 and dissolved nitrogen were found in high mountain lakes only; however, these correlations were weak ($-0.75 < \text{cor} < 0.75$; Table S4). No significant correlations with temperature were detected.

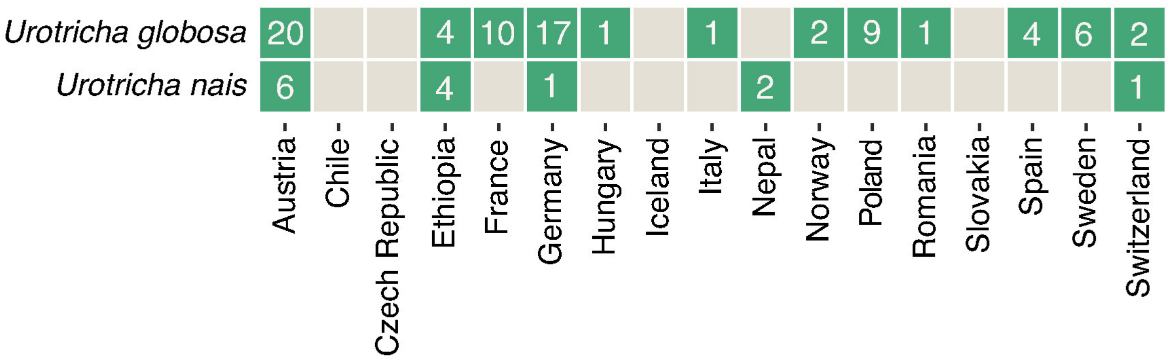

Figure 8. Distribution of the two *Urotricha* strains. Green squares indicate the occurrence of V4- and V9-markers in a country and the numbers indicate in how many lakes they were found per country. Detailed information about the investigated freshwater lakes can be found in Table S1 and [1].

4. Discussion

Urotricha species occur worldwide in various aquatic freshwater systems, and their key role as grazers on phytoplankton has been elucidated [1,3,33]. About 40 species have been described so far and although their overall feeding trait and probably also their correlation to certain environmental parameters are similar, some species were obviously found in

colder habitats and regions of the world [4–8,10]. However, although the two species that we isolated originated from high mountain lakes, they were also found in water bodies located on several continents, as elucidated from sequences detected in worldwide HTS datasets and records of 'environmental sequences' in public databases. However, from our investigated abiotic datasets, we could not find any significant correlations with water temperature and, therefore, we have to reject our initial hypothesis that these species are presumably cold-adapted species preferring the cooler waters of high mountain lakes.

However, it was very challenging finding already described morphotypes to which the two urotrich isolates could be assigned to. Based on the available original descriptions and re-descriptions of small urotrichs that typically have one caudal cilium and extrusomes, we were not able to unambiguously identify the here investigated species (Table 2). We faced two possibilities how to handle and justify the 'species assignment problem': either we reconciled the two urotrichs with the *U. agilis* complex because, therein, several genetically different urotrichs having a very similar morphology were merged, or, we kept our species apart from the *U. agilis* complex because of some specific special features, e.g., the extrusomes in the oral region and in the unciliated posterior portion in *U. globosa* or the cold habitat. Currently, we are unable to provide a final assignment and, therefore, we decided to treat the two urotrichs as separate species until future studies might shed more light on this difficult issue.

Table 2. Comparison of the main characteristics among the *Urotricha* strain CIL-2017/19 from Lake Faselfad, the natural *Urotricha* population from Lake Hairlach, the *Urotricha agilis* complex, *Urotricha nais*, *Urotricha globosa*, *Urotricha ristoi*, *Urotricha ovata* and *Urotricha farcta* based on stained material if not indicated otherwise. 'n.d.' not determined, '-' not present, * observed only in very few specimens (n = 2–5).

Characteristic	*U. nais* Lake Faselfad	*U. globosa* Lake Hairlach	*U. agilis* Complex	*U. nais*	*U. globosa*	*U. ristoi*	*U. ovata*	*U. farcta*
Size range (length × width), µm, in vivo	17–35 × 15–29	n.d.	13–23 × 9–16	n.d.	18–24 × 15–25	15–25 × 10–25	25–40 × 20–38	15–30 × 15–25
Size range (length × width), µm	10–18 × 8–14	11–17 × 9–15	9–16 × 6–14	16–34 × 12–32	*	12–18 × 10–20	*	*
Somatic kineties, number	15–19	16–24	14–24	18–21	17–25	25–28	19–27	20–30
Cilia in a somatic kinety, number	8–11	5–8	5–11	5–11	13–15	9–14	ca. 19	10–16
Circumoral dikinetids, number	n.d.	8–13	8–9	9–10	11–13	5–6	ca. 10	10–14
Adoral organelles, number	2 *	2 *	3	2	3	2	3	2–3
Adoral organelle 1, dikinetid number	3–4	4	3–5	4	n.d.	4	n.d.	3–4
Adoral organelle 2, dikinetid number	2	2	2–3	2	n.d.	4	n.d.	3–4
Adoral organelle 3, dikinetid number	-	-	1–2	-	n.d.	-	n.d.	2
Extrusomes present	yes	yes	yes	yes	yes	'not seen'	yes	yes
Extrusomes, length, µm	1.0–2.7	1.0–1.5	1.0–1.5	n.d.	short	-	1.5–2.0	1.5–2.0
Reference	This study	This study	[1]	[34]	[35]	[36]	[37]	[13]

Comparison of the Two Urotricha Species with Congeners

For the comparison of the here investigated two urotrich isolates with morphologically similar species, we considered only described species with one caudal cilium, <40 µm in length, <30 somatic kineties, <20 cilia in an unshortened somatic kinety, most probably extrusomes and 2–3 adoral organelles (Table 2). Due to their tininess, we cannot exclude that our two species investigated here might have more than two adoral organelles that were simply not seen in our protargol stained specimens.

From morphology, the *Urotricha* from Lake Hairlach is almost indistinguishable from specimens of the *U. agilis* complex (Table 2). However, the (vertical) pattern of the extrusomes in the unciliated posterior portion and the specific extrusomes found only in the oral region (Figures 1 and 2) distinguish these urotrichs from the descriptions given in [1]. We then compared relatively stable morphological features among the urotrichs presented in Table 2 and decided to assign it to *U. globosa* having a similar number of somatic kineties, i.e., 16–24 and 17–25 despite some differences in the number of cilia in one somatic kinety, i.e., 5–8 vs. 13–15. However, the latter feature overlaps more conveniently for the *Urotricha*

from Lake Faselfad with *U. nais*, i.e., 8–11 vs. 5–11 and here, the number of somatic kineties also match, i.e., 15–19 vs. 18–21; we therefore tentatively assigned this morphotype to *U. nais*. As with *U. globosa* from Lake Hairlach, *U. nais* is, again, morphologically very similar to the *U. agilis* complex.

Generally, planktonic *Urotricha* species frequently appear in freshwater worldwide and often dominate planktonic ciliate communities [1,2,10,13,14,38,39]. In temperate lakes in spring, some urotrichs, together with other prostomatid and oligotrich ciliates, have a significant grazing impact on the phytoplankton bloom [2,38,40]. Interestingly, although urotrichs have a central role in microbial food webs [3], only a few new species have been described in the past decades [14,41,42]. Studies including molecular sequences are virtually non-existent except for the ones observed in Frantal et al. [1], Qu et al. [3] and the two species studied here. However, as these ciliates play a significant role in planktonic food webs, it is important, especially in respect to metabarcoding studies, that their molecular sequences are properly identified, i.e., naming and depositing them in public databases. In our biogeographic approach to trace back *U. nais* and *U. globosa*, we showed that it is still possible to reveal species-specific distribution patterns from previously 'nameless' environmental sequencing datasets.

Supplementary Materials: The following supporting information can be downloaded at: https://www.mdpi.com/article/10.3390/d14050362/s1, Figure S1: SSU rDNA phylogeny of 23 prostomatean taxa; Figure S2: V9 secondary structures of the investigated *Urotricha* strains; Table S1: Biogeographic screening; Table S2: Morphometric table; Table S3: HTS records of *Urotricha globosa* and *Urotricha nais* based on V4 and V9 similarity; Table S4: Spearman correlations of the urotrichs with environmental parameters.

Author Contributions: Conceptualization, B.S. and T.P.; data curation, B.S. and T.P.; formal analysis, S.F.; funding acquisition, B.S. and T.S.; investigation, B.S., D.F., B.K., T.D., S.F., T.S., M.G. and T.P.; methodology, B.S., T.D., S.F., T.S., M.G. and T.P.; project administration, B.S. and T.S.; writing—original draft, B.S. and T.P.; writing—review and editing, D.F, B.K., T.D., S.F., T.S. and M.G. All authors have read and agreed to the published version of the manuscript.

Funding: This research was funded by the Austrian Science Fund FWF, grant numbers P21013-B03 (B.S.), I2238-B25 (B.S.), V233-B17 (Barbara Tartarotti). T.S. received funding from the Deutsche-Forschungsgemeinschaft (STO414/13-3). B.K. was funded by a Doctoral Fellowship of the Austrian Academy of Sciences (OEAW, DOC-fForte 22883).

Institutional Review Board Statement: Not applicable.

Informed Consent Statement: Not applicable.

Data Availability Statement: Not applicable.

Acknowledgments: We thank Josef Franzoi, Claudia Grubbauer, Gry Larsen, Salvador Morales-Gomez, Ulrike Scheffel, Kathrin Schwab, Monika Summerer and Florian Trattner for their help during sampling and in the laboratory. The samples from Lake Hairlach were collected by the Ecology Department of the University of Innsbruck; the samples from Lake Faselfad by B.K. We dedicate this publication to our respected Ukrainian and Russian colleagues. Open Access Funding by the Austrian Science Fund (FWF).

Conflicts of Interest: The authors declare no conflict of interest.

References

1. Frantal, D.; Agatha, S.; Beisser, D.; Boenigk, J.; Darienko, T.; Dirren-Pitsch, G.; Filker, S.; Gruber, M.; Kammerlander, B.; Nachbaur, L.; et al. Molecular data reveal a cryptic diversity in the genus *Urotricha* (Alveolata, Ciliophora, Prostomatida), a key player in freshwater lakes, with remarks on morphology, food preferences, and distribution. *Front. Microbiol.* **2022**, *12*, 787290. [CrossRef] [PubMed]
2. Müller, H.; Schöne, A.; Pinto-Coelho, R.M.; Schweizer, A.; Weisse, T. Seasonal succession of ciliates in Lake Constance. *Microb. Ecol.* **1991**, *21*, 119–138. [CrossRef] [PubMed]

3. Qu, Z.; Forster, D.; Bruni, E.P.; Frantal, D.; Kammerlander, B.; Nachbaur, L.; Pitsch, G.; Posch, T.; Pröschold, T.; Teubner, K.; et al. Aquatic food webs in deep temperate lakes: Key species establish through their autecological versatility. *Mol. Ecol.* **2021**, *30*, 1053–1071. [CrossRef]
4. Wille, A.; Sonntag, B.; Sattler, B.; Psenner, R. Abundance, biomass and size structure of the microbial assemblage in the high mountain lake Gossenköllesee (Tyrol, Austria) during the ice-free period. *J. Limnol.* **1999**, *58*, 117–126. [CrossRef]
5. Sonntag, B.; Summerer, M.; Sommaruga, R. Factors involved in the distribution pattern of ciliates in the water column of a transparent alpine lake. *J. Plankton Res.* **2011**, *33*, 541–546. [CrossRef]
6. Sonntag, B.; Kammerlander, B.; Summerer, M. Bioaccumulation of ultraviolet sunscreen compounds (mycosporine-like amino acids) by the heterotrophic freshwater ciliate *Bursaridium* living in alpine lakes. *Inland Waters* **2017**, *7*, 55–64. [CrossRef]
7. Kammerlander, B.; Koinig, K.A.; Rott, E.; Sommaruga, R.; Tartarotti, B.; Trattner, F.; Sonntag, B. Ciliate community structure and interactions within the planktonic food web in two alpine lakes of contrasting transparency. *Freshwat. Biol.* **2016**, *61*, 1950–1965. [CrossRef]
8. Sommer, F.; Sonntag, B.; Rastl, N.; Summerer, M.; Tartarotti, B. Ciliates in man-made mountain reservoirs. *Front. Microbiol.* 2022; *under revision*.
9. Rose, K.C.; Williamson, C.E.; Saros, J.E.; Sommaruga, R.; Fischer, J.M. Differences in UV transparency and thermal structure between alpine and subalpine lakes: Implications for organisms. *Photochem. Photobiol.* **2009**, *8*, 1244–1256. [CrossRef]
10. Kammerlander, B.; Breiner, H.W.; Filker, S.; Sommaruga, R.; Sonntag, B.; Stoeck, T. High diversity of protistan plankton communities in remote high mountain lakes in the European Alps and the Himalayan mountains. *FEMS Microbiol. Ecol.* **2015**, *91*, fiv010. [CrossRef]
11. Foissner, W. An update of 'basic light and scanning electron microscopic methods for taxonomic studies of ciliated protozoa'. *Int. J. Syst. Evol. Microbiol.* **2014**, *64*, 271–292. [CrossRef]
12. Skibbe, O. An improved quantitative protargol stain for ciliates and other planktonic protists. *Arch. Hydrobiol.* **1994**, *130*, 339–347. [CrossRef]
13. Foissner, W.; Berger, H.; Kohmann, F. *Taxonomische und Ökologische Revision der Ciliaten des Saprobiensystems. Band III: Hymenostomata, Prostomatida, Nassulida. Informationsber. Bayer*; Landesamt für Wasserwirtschaft: Munich, Germany, 1994; Volume 1/94, pp. 1–548.
14. Foissner, W.; Berger, H.; Schaumburg, J. *Identification and Ecology of Limnetic Plankton Ciliates. Informationsber. Bayer*; Landesamt für Wasserwirtschaft: Munich, Germany, 1999; Volume 3/99, pp. 1–793.
15. Swofford, D.L. *PAUP* Phylogenetic Analysis Using Parsimony (*and Other Methods), Version 4.0b10*; Sinauer Associates: Sunderland, MA, USA, 2002.
16. Stamatakis, A. RAxML version 8: A tool for phylogenetic analysis and post-analysis of large phylogenies. *Bioinformatics* **2014**, *30*, 1312–1313. [CrossRef] [PubMed]
17. Jow, H.; Hudelot, C.; Rattray, M.; Higgs, P. Bayesian phylogenetics using an RNA substitution model applied to early mammalian evolution. *Mol. Biol. Evol.* **2002**, *19*, 1591–1601. [CrossRef]
18. Higgs, P.; Jameson, D.; Jow, H.; Rattray, M. The evolution of tRNA-Leu genes in animal mitochondrial genomes. *J. Mol. Evol.* **2003**, *57*, 435–445. [CrossRef] [PubMed]
19. Hudelot, C.; Gowri-Shankar, V.; Jow, H.; Rattray, M.; Higgs, P. RNA-based phylogenetic methods: Application to mammalian mitochondrial RNA sequences. *Mol. Phylogen. Evol.* **2003**, *28*, 241–252. [CrossRef]
20. Gibson, A.; Gowri-Shankar, V.; Higgs, P.; Rattray, M. A comprehensive analysis of mammalian mitochondrial genome base composition and improved phylogenetic methods. *Mol. Biol. Evol.* **2005**, *22*, 251–264. [CrossRef]
21. Telford, M.J.; Wise, M.J.; Gowri-Shankar, V. Consideration of RNA secondary structure significantly improves likelihood-based estimates of phylogeny: Examples from the bilateria. *Mol. Biol. Evol.* **2005**, *22*, 1129–1136. [CrossRef] [PubMed]
22. Zuker, M. Mfold web server for nucleic acid folding and hybridization prediction. *Nucleic Acid Res.* **2003**, *31*, 3406–3615. [CrossRef]
23. Byun, Y.; Han, K. PseudoViewer. Web application and web service for visualizing RNA pseudoknots and secondary structures. *Nucleic Acids Res.* **2006**, *34*, W416–W422. [CrossRef]
24. Do, C.B.; Woods, D.A.; Batzoglou, S. CONTRAfold: RNA secondary structure prediction without physics-based models. *Bioinformatics* **2006**, *22*, e90–e98. [CrossRef]
25. Coleman, A.W. ITS2 is a double-edged tool for eukaryote evolutionary comparisons. *Trends Genet.* **2003**, *19*, 370–375. [CrossRef]
26. Coleman, A.W. Pan-eukaryote ITS2 homologies revealed by RNA secondary structure. *Nucleic Acids Res.* **2007**, *35*, 3322–3329. [CrossRef] [PubMed]
27. Cote, C.A.; Greer, C.L.; Peculis, B.A. Dynamic conformational model for the role of ITS2 in pre-rRNA processing in yeast. *RNA* **2002**, *8*, 786–797. [PubMed]
28. Coleman, A.W. *Paramecium aurelia* revisited. *J. Eukaryot. Microbiol.* **2005**, *52*, 68–77. [CrossRef] [PubMed]
29. Darienko, T.; Gustavs, L.; Eggert, A.; Wolf, W.; Pröschold, T. Evaluating the species boundaries of green microalgae (*Coccomyxa*, Trebouxiophyceae, Chlorophyta) using integrative taxonomy and DNA barcoding with further implications for the species identification in environmental samples. *PLoS ONE* **2015**, *10*, e0127838. [CrossRef]
30. Boenigk, J.; Wodniok, S.; Bock, C.; Beisser, D.; Hempel, C.; Grossmann, L.; Lange, A.; Jensen, M. Geographic distance and mountain range structure freshwater protist communities on a European scale. *Metabarcoding Metagenom.* **2018**, *2*, e21519. [CrossRef]

31. Oikonomou, A.; Filker, S.; Breiner, H.-W.; Stoeck, T. Protistan diversity in a permanently stratified meromictic lake (Lake Alatsee, SW Germany). *Environ. Microbiol.* **2015**, *17*, 2144–2157. [CrossRef]
32. Filker, S.; Sommaruga, R.; Vila, I.; Stoeck, T. Microbial eukaryote plankton communities of high-mountain lakes from three different continents exhibit strong biogeographic patterns. *Mol. Ecol.* **2016**, *25*, 2286–2301. [CrossRef]
33. Weisse, T.; Karstens, N.; Meyer, V.C.L.; Janke, L.; Lettner, S.; Teichgräber, K. Niche separation in common prostome freshwater ciliates: The effect of food and temperature. *Aquat. Microb. Ecol.* **2001**, *26*, 167–179. [CrossRef]
34. Muñoz, A.; Téllez, C.; Fernández-Galiano, D. Morphology and infraciliature in *Urotricha nais* sp. n. and *Urotricha castalia* sp. n. (Ciliophora, Prorodontida). *Acta Protozool.* **1987**, *26*, 197–204.
35. Song, W.; Wilbert, N. Taxonomische Untersuchungen an Aufwuchsciliaten (Protozoa, Ciliophora) im Poppelsdorfer Weiher, Bonn. *Lauterbornia* **1989**, *3*, 2–221.
36. Krainer, K.-H. Taxonomische Untersuchungen an neuen und wenig bekannten planktischen Ciliaten (Protozoa: Ciliophora) aus Baggerseen in Österreich. *Lauterbornia* **1995**, *21*, 39–68.
37. Foissner, W. Ecological and systematic studies on the neuston of alpine pools, with special regard to ciliated protozoa. *Int. Revue Ges. Hydrobiol.* **1979**, *64*, 99–140. [CrossRef]
38. Sonntag, B.; Posch, T.; Klammer, S.; Teubner, K.; Psenner, R. Phagotrophic ciliates and flagellates in an oligotrophic, deep, alpine lake: Contrasting variability with seasons and depths. *Aquat. Microb. Ecol.* **2006**, *43*, 193–207. [CrossRef]
39. Sichrowsky, U.; Schabetsberger, R.; Sonntag, B.; Stoyneva, M.; Maloney, A.E.; Nelson, D.B.; Richey, J.N.; Sachs, J.P. Limnological characterization of volcanic crater lakes on Uvea Island (Wallis and Futuna, South Pacific). *Pac. Sci.* **2014**, *68*, 333–343. [CrossRef]
40. Sommaruga, R.; Psenner, R. Nanociliates of the order Prostomatida: Their relevance in the microbial food web of a mesotrophic lake. *Aquat. Sci.* **1993**, *55*, 179–187. [CrossRef]
41. Sonntag, B.; Foissner, W. *Urotricha psenneri* n. sp. and *Amphileptus piger* (Vuxanovici, 1962) n. comb., two planktonic ciliates (Protozoa, Ciliophora) from an oligotrophic lake in Austria. *J. Eukaryot. Microbiol.* **2004**, *51*, 670–677. [CrossRef]
42. Foissner, W. *Urotricha spetai* nov. spec., a new plankton ciliate (Ciliophora, Prostomatea) from a fishpond in the Seidlwinkel Valley, Rauris, Austrian Central Alps. *Verh. Zool.-Bot.-Ges. Österreich* **2012**, *148/149*, 173–184.